Lawrence Berkeley Laboratory
UNIVERSITY OF CALIFORNIA

Materials & Molecular Research Division

Presented at the XVIIth International Conference on Low Temperature Physics, Karlsruhe, West Germany, August 15-22, 1984

ULTRASENSITIVE MEASURING DEVICES

J. Clarke

August 1984

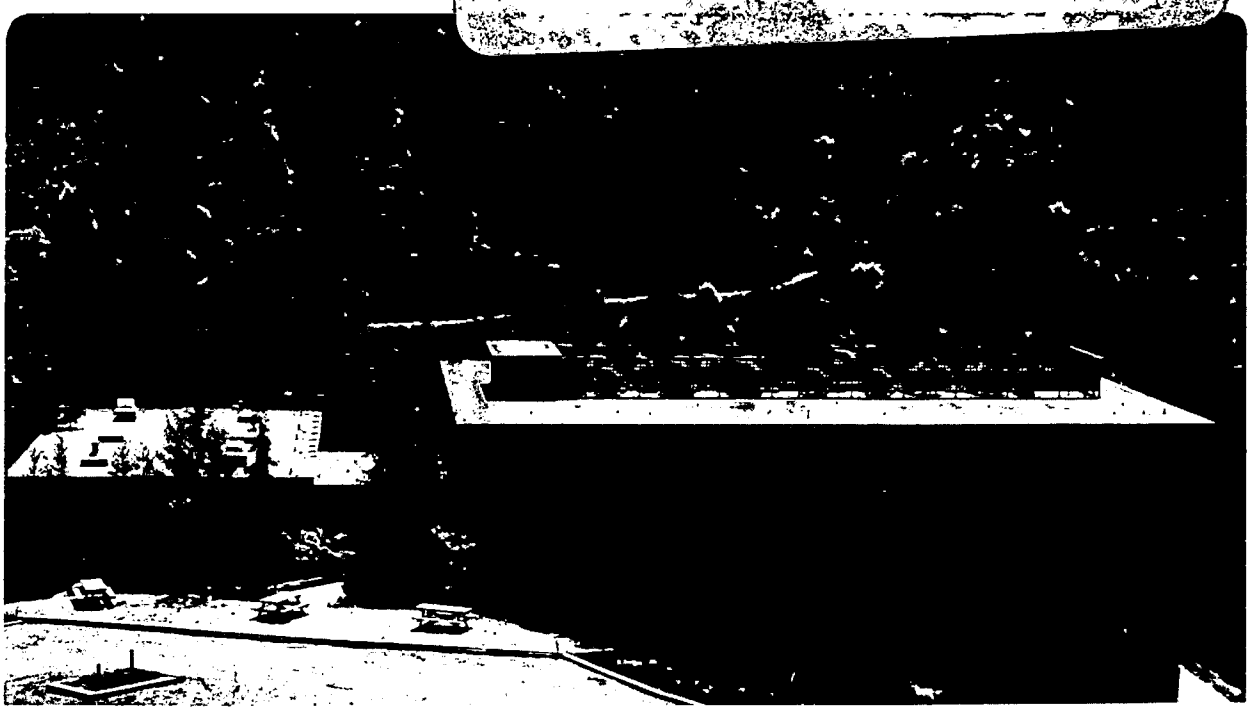

Prepared for the U.S. Department of Energy under Contract DE-AC03-76SF00098

DISCLAIMER

ULTRASENSITIVE MEASURING DEVICES

John CLARKE

Department of Physics, University of California, and Materials and Molecular Research Division, Lawrence Berkeley Laboratory, Berkeley, California 94720

Both dc and rf Superconducting QUantum Interference Devices (SQUIDs) are widely used as ultrasensitive detectors of magnetic flux. Present research is focussed largely on thin-film dc SQUIDs fabricated with photolithographic techniques. The current status of this field is briefly reviewed. The impact of dc SQUIDs with improved sensitivity on noise thermometry and gravitational wave antennas is discussed.

1. INTRODUCTION

The dc SQUID [Superconducting QUantum Interference Device (1)] first appeared in 1964. Its potential as a very sensitive detector of magnetic flux, and hence of many other physical quantities, was quickly realized, and for several years it was used in a variety of cryogenic experiments. However, in 1970 the rf SQUID appeared (2), and, probably because it involved only a single Josephson junction (3) instead of the two required by the dc SQUID, became commercially available shortly thereafter. Thus, for a substantial period of time, there was comparatively rapid development of the rf SQUID, with little attention paid to the dc SQUID. In the mid-70's, however, this situation was reversed when it became apparent that the dc SQUID was potentially much more sensitive than the rf SQUID (4). This realization, together with the maturing of thin-film technology that made it no more difficult to make two junctions than one, has led to an extensive development of the dc SQUID, particularly over the past five years or so. Thus, the sensitivity of rf SQUIDs has not changed greatly over the past decade while that of dc SQUIDs has improved by several orders of magnitude. Despite the much higher sensitivity of the dc SQUID, however, there is little doubt that the rf SQUID is by far the more widely used of the two devices. This is partly a result of the fact that the rf SQUID has adequate sensitivity for many applications, but probably mostly because dc SQUIDs have become commercially available only very recently. In this brief review, I will concentrate on developments relating to the dc SQUID.

2. THE DC SQUID

2.1 Principles of Operation

The dc SQUID is shown schematically in Fig. 1(a). The two Josephson junctions have critical current I_o and self-capacitance C. To eliminate hysteresis on the current-voltage (I-V) characteristic one needs to add an external shunt resistance R such that $\beta_C = 2\pi I_o R^2 C/\Phi_o \lesssim 1$. The inductance of the superconducting loop is L. In normal operation, one biases the SQUID with a constant current I_B so that a voltage appears across it [Fig. 1(b)], and measures the change in voltage induced by a small change in the magnetic flux threading the SQUID loop. As the magnetic flux Φ is slowly varied, the I-V characteristic oscillates between the two extrema shown in Fig. 1(b), with a period of one flux quantum, $\Phi_o = h/2e = 2 \times 10^{-15}$ Wb. Correspondingly, the voltage at constant bias current oscillates with magnetic flux as indicated in Fig. 1(c). Thus, the SQUID is, in essence, a flux-to-voltage transducer with a transfer function $V_\Phi = (\partial V/\partial \Phi)_I$ that is a maximum when the quasi-state flux in the SQUID is near $(2n + 1)\Phi_o/4$, where n is an integer. In most applications at frequencies below, say 100 kHz, the SQUID is operated in a flux-locked loop. An oscillating flux is applied to the SQUID and the resulting voltage that is generated across the SQUID is amplified by a cooled transformer or resonant circuit and then by an amplifier. The signal from the amplifier is lock-in detected and the output from the lock-in fed back into a coil

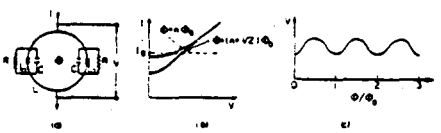

FIGURE 1
(a) Configuration of dc SQUID; (b) I-V characteristic with $\Phi = n\Phi_o$ and $(n + 1/2)\Phi_o$; (c) V vs. Φ at constant bias current.

coupled to the SQUID. When a magnetic flux change $\delta\Phi$ is applied to the SQUID, the feedback circuit produces an equal, opposing flux and a corresponding output voltage that is proportional to $\delta\Phi$.

In virtually all practical applications, the SQUID is coupled to a superconducting input coil, and is thus converted into a galvanometer. In this configuration, the SQUID can be used to measure a variety of physical quantities, for example, magnetic field, magnetic field gradient, magnetic susceptibility, voltage, gravity gradients, and displacement.

Although the principles of operation have been known for two decades, there have been major changes in the design of dc SQUIDs in the past few years, with correspondingly major improvements in sensitivity. To explain the reasons for these advances, we now briefly review the origins of noise in the SQUID.

2.2. Noise Theory

To calculate the smallest detectable change in magnetic flux we need to know the voltage noise across the SQUID and the transfer function, V_Φ. Leaving aside the issue of 1/f noise at low frequencies for the moment, we assume that the only sources of noise are the Johnson current noises in the two resistive shunts with spectral density $4k_BT/R$ at temperature T. These noise sources produce a voltage noise across the SQUID with spectral density $S_V(f)$, and also a current noise around the SQUID loop with spectral density $S_J(f)$. Numerical simulations for a SQUID that is optimized for low noise ($\beta = 2LI_o/\Phi_o = 1$, $\beta_C \lesssim 1$) in the He^4 temperature range show that (5)

$$V_\Phi = R/L \qquad (1)$$

and

$$S_V(f) = 16k_BTR. \qquad (2)$$

If we can detect a flux change $\delta\Phi$ in the SQUID, we can associate with it an energy $(\delta\Phi)^2/2L$. This leads to a convenient parameter to characterize the noise of a SQUID, the equivalent flux noise energy per unit bandwidth, $\varepsilon/1Hz = S_V(f)/2LV_\Phi^2$. Using this expression and Eqs. (1) and (2), one can easily show that

$$\varepsilon/1Hz = 9k_BTL/R = 16k_BT(LC)^{1/2}, \qquad (3)$$

where the last expression assumes $\beta = \beta_C = 1$. Although the numerical factors are somewhat model dependent, Eq. (3) gives a clear-cut prescription for reducing $\varepsilon/1Hz$, that is, for improving the sensitivity. Thus, one should design the SQUID to have the lowest values of L and C possible. One should bear in mind, however, that it becomes difficult to couple a SQUID to an input coil of useful dimensions if L becomes too small. Equation (3) also shows that the noise energy scales with T, but one should be aware that at temperatures below about 1K the noise of the amplifier folowing the SQUID is likely to become dominant.

Needless to say, one does not expect to be able to reduce the sensitivity indefinitely -- eventually, quantum mechanical effects should impose a limitation. A theory (6) has been developed in which, in the limit $T \to 0$, the Nyquist noise in the shunt resistors is replaced by zero point fluctuations with a current spectral density $2h\nu/R$ at frequency ν. Numerical simulations have shown that for an optimized SQUID the minimum noise energy is $\varepsilon/1Hz \sim h$. However, it should be emphasized that there appears to be no precise quantum mechanical limit on the noise energy itself (7). As we shall see in Sec. 3.3, two noise sources are needed to specify the performance of an amplifier, and a fundamental limit applies to an appropriate combination of these two sources.

2.3. Practical SQUIDs

The first tunnel junction dc SQUID (4) on which systematic noise measurements were made (in 1976) in fact predated the development of the noise theory outlined above. The device was fabricated from thin films deposited through metal masks, and had an inductance of about 1 nH. The area of the Nb-NbOx-Pb tunnel junctions was about 10^4 μm^2. The noise energy at 4.2K, about 3×10^{-30} J Hz^{-1} (3×10^4 h) at frequencies above the 1/f noise region, was within a factor of 3 of the prediction of Eq. (3).

It became clear that major improvements in sensitivity would involve devices with much smaller dimensions. The subsequent progress in fabrication has been largely a result of the technology pioneered at IBM in the Josephson computer project (8). All of the most sensitive SQUIDs rely on photolithography or even electron-beam lithography to produce narrow lines or small windows. The junction areas are typically a few microns square, and the barriers are prepared either by thermal oxidation or, increasingly, by a rf discharge in an $Ar-O_2$ mixture (8). Some of the earlier devices relied on Pb alloy technology throughout, while others have been made largely from Nb with Nb-NbOx-Pb tunnel junctions. A few devices have been made entirely from Nb. The Nb-based devices have proved particularly reliable with respect to storage and thermal cycling.

In this short article, it is impossible to describe the wide variety of devices that have been fabricated. However, to give an idea of the advances in sensitivity that have resulted from the microfabrication technology in recent years, in Fig. 2 we plot the measured noise energies of a selection of devices vs. the predicted values. In all cases, the SQUIDs were surrounded by a superconducting shield to eliminate external magnetic field fluctuations. The solid line represents exact agreement between theory and experiment. Although there is

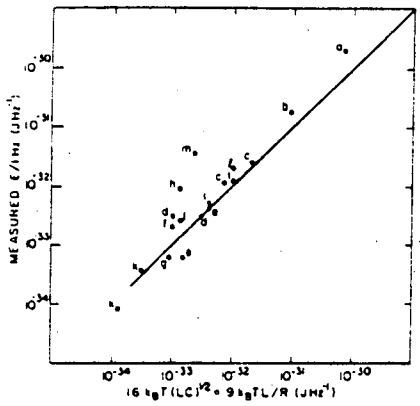

FIGURE 2

Measured and predicted values of ε/1Hz for a selection of dc SQUIDs with tunnel junctions (except f, which involved microbridges). In the case of k, the 1/f noise has been subtracted. The SQUIDs were operated at the temperatures listed and are described in the following references:

a	4.2K (4)	h	4.2K (14)
b	4.2K (9)	i	4.2K, 1.5K (14)
c	4.2K, 1.6K (10)	j	4.2K (15)
d	4.2K, 1.8K (11)	k	4.2K, 1.4K (16)
e	4.2K, 1.5K (12)	ℓ	4.2K (17)
f	4.2K (12)	m	4.2K (18)
g	4.2K (13)		

a good deal of scatter in the data, nonetheless one sees that Eq. (3) is an adequate prediction of the noise energy. It is evident that the noise energy has been improved by more than 4 orders of magnitude by appropriate design. The smallest noise energy represented in Fig. 2 is about ħ, although this value represents the residual white noise energy after a 1/f noise contribution (~ 2ħ) had been subtracted out (16). Thus, it appears that the noise energy of this device was rather close to the limit imposed by zero point fluctuations. The SQUID used in these measurements had very low inductance, about 2 pH, and is therefore difficult to couple efficiently to most input circuits that typically have inductances of the order of 1 μH.

For applications in which the input circuit is untuned, the energy sensitivity referred to the input scales as $1/\alpha^2$ and is thus seriously degraded unless the coupling is efficient, that is, α^2 approaches unity (19). This problem has received considerable attention. A major advance was made by Dettmann et al. (20) and Ketchen and Jaycox (13) who fabricated planar devices with a thin-film input coil deposited over the body of the SQUID (but insulated from it) so that the SQUID provided a superconducting groundplane for the coil. The groundplaning effect not only greatly reduces the inductance of the input coil compared with its free-standing value, but also ensures very tight coupling of magnetic flux between the input coil and the SQUID. An alternative scheme for efficient coupling has been developed by Carelli and Foglietti (15), who developed a "fractional-turn" dc SQUID with many loops in parallel across two tunnel junctions.

A version of the SQUID based on the former scheme and fabricated at Berkeley is shown in Fig. 3. The devices are fabricated using photolithographic patterning in batches of 9 on 50 mm oxidized silicon wafers. The body of the SQUID and the spiral input coil are of Nb, while the counter-electrode for the two Josephson junctions is a Pb alloy. Typical parameters for this device with a 50-turn coil are as follows: $L \approx 0.4$ nH, $I_0 \approx 5$ μA, $R \approx 8$ Ω, inductance of input coil, $L_i \approx 0.8$ nH, and $\alpha^2 = M_i^2/L_i L \approx 0.8$ (M_i is the mutual inductance between the SQUID and the input coil). At 4.2K, the rms flux noise in a flux-locked loop was about 2×10^{-6} Φ_0 $Hz^{-1/2}$, corresponding to ε/1Hz ≈ 200ħ. In a flux-locked loop designed to have a fast response, a frequency response of 70 kHz (± 3 dB), a maximum slew rate of 3×10^6 Φ_0 s^{-1} (at 6 kHz) and a dynamic range of $\pm 2 \times 10^7$ in a unit bandwidth were achieved (21). The quoted sensitivity appears to be representative of what is currently achievable for a tightly coupled SQUID in a flux-locked loop, although somewhat higher sensitivities have been reported for well-coupled devices that are operated in an open-loop configuration without feedback (14,15).

2.4. 1/f Noise

The SQUID just described exhibits a flux noise spectral density proportional to 1/f (f is the frequency) at low frequencies, in this case typically below about 10 Hz. All SQUIDs in which the low frequency noise has been measured show the same phenomenon, which imposes a serious limitation on the low frequency sensitivity of SQUIDs. The origin of the 1/f noise is not at all well understood. A single Josephson tunnel junction exhibits 1/f noise in its critical current which has recently been shown to arise from traps in the tunnel junction (22,23), but in most (but not necessarily all) SQUIDs this noise is much too small to account for the observed 1/f flux noise. In a collection of 5 types of SQUIDs investigated at Berkeley (24) with a very wide range of parameters, for example, a three-order-magnitude spread in both L and C, it was found that the 1/f flux noise spectral density was always within a factor of 3 of $10^{-10}/(f/1\text{Hz})\Phi_0^2$ Hz^{-1}. However, very recently SQUIDs have been operated with substantially lower levels of 1/f noise (25), although the reason for the improved performance seems far

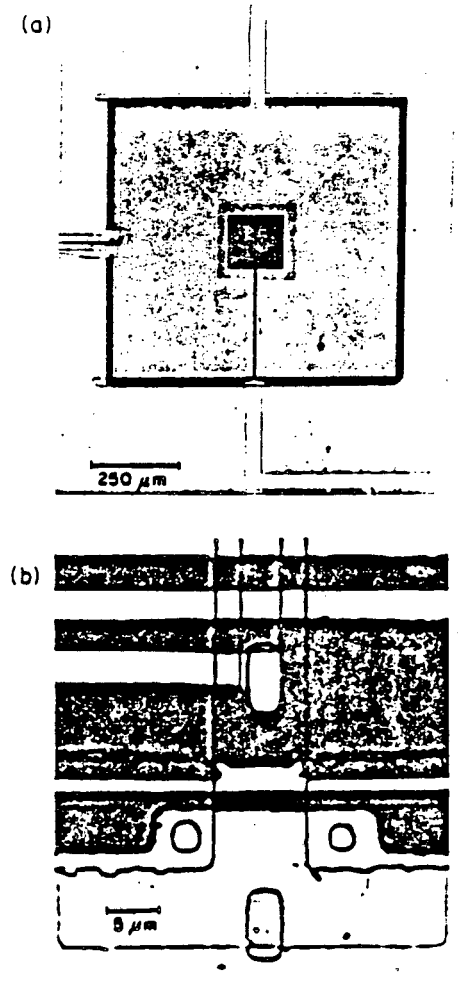

FIGURE 3
(a) Photograph of planar dc SQUID with 50-turn input coil; (b) photograph showing junctions and resistive shunt.

from clear. It is possible that the 1/f noise arises from the motion of flux trapped in the body of the SQUID, and that the magnitude of the noise depends critically on the fabrication technology or on the amount of flux trapped when the SQUID is cooled. This is clearly an area where more research is needed.

3. THE DC SQUID AS AN INSTRUMENT

SQUIDs have been incorporated into a wide variety of instruments. In this section, we describe briefly three very different, recent examples that illustrate the impact of photolithographic techniques on the field.

3.1. Thin-Film Gradiometers

Magnetic gradiometers are used to measure gradients of an externally applied magnetic field, usually the first or second derivative. For example, a gradiometer to measure the diagonal component $\partial H_z/\partial z$ consists of two coaxial, spatially separated superconducting loops of equal area wound in opposition to each other and connected in series with the input coil of a SQUID. Thus, a uniform applied magnetic field links no magnetic flux to the circuit, while a change in the magnetic field gradient along the axis of the loops produces a net flux proportional to the gradient, and a corresponding current in the input coil of the SQUID. Second-derivative gradiometers, in particular, are of considerable importance in biomagnetic applications because they are sensitive to a weak, locally generated fields with a high gradient while discriminating strongly against background magnetic fluctuations that have rather small second derivatives (26).

Although most practical gradiometers involve wire-wound pick-up loops, thin-film planar gradiometers that measure either first (27,28) or second derivatives (29) have been successfully operated. As an example, we briefly describe the device of de Waal *et al.* (28), shown in Fig. 4, that measures an off-diagonal component, for

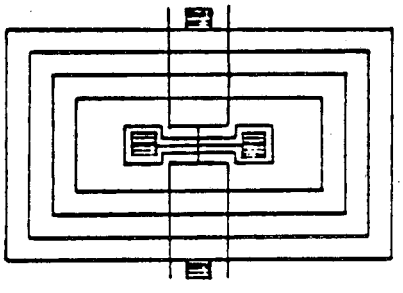

FIGURE 4
Thin film, first-derivative gradiometer (from Ref. 28).

example, $\partial H_z/\partial x$. The overall length is 16.5 mm. Each overlap of two lines represents a superconducting connection. Two tunnel junctions (not visible in the drawing) are located in series on the central, vertical line, one on each side of the central, horizontal line. Thus, the device is, in essence, a "two-hole dc SQUID", with five pairs of pick-up loops connected in parallel. The inductance of the SQUID is determined largely by the smallest loops, while the signal is detected largely by the larger loops. The measured sensitivity of the gradiometer is about 3×10^{-12} T m^{-1} Hz$^{-1/2}$, and, for example, is ade-

quate for magnetocardiology. The intrinsic balance of the device is 300 ppm. The balance was improved by adding a SQUID magnetometer to the system, and adding an appropriate fraction of the magnetometer output to the gradiometer output to reduce the sensitivity to magnetic field and thus improve the balance to 20 ppm. This technique, sometimes called "dynamic balancing" is commonly used to improve the balance of gradiometers.

It seems likely that there will be considerable effort in the near future to develop thin-film gradiometers, particularly for the investigation of spontaneous and evoked brain activity for which large arrays of sensors are highly desirable. However, it will be necessary to make several advances on the system just described. For most applications, it is necessary to use a second-derivative axial gradiometer, that is, one that measures $\partial^2 H_z/\partial z^2$. Such a device is necessarily three-dimensional (rather than planar), a considerable although not insurmountable complication. Furthermore, a higher sensitivity is required: This could probably be achieved by coupling the pick-up loops to a spiral input coil, thereby optimizing the energy transfer to the SQUID.

3.2. Miniature SQUID Susceptometer

Ketchen et al. (30) have described a thin-film susceptometer capable of studying the magnetic susceptibility of micron-sized particles. The device is shown schematically in Fig. 5.

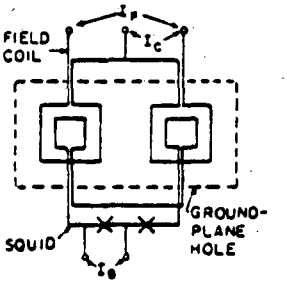

FIGURE 5
Thin film susceptometer (from Ref. 30).

The dc SQUID is constructed as a planar gradiometer, each loop being 17.5 μm across with an inductance of about 30 pH. A magnetic field may be applied to the two loops by means of the current I_F in the field coil. The field in each loop can be adjusted to give zero response from the SQUID by means of a resistive divider connected to the center top of the field coil. If a particle is placed in one pick-up loop, however, the SQUID will detect an out-of-balance signal when a magnetic field is applied that is proportional to the susceptibility of the particle. As a test of the system, the magnetic flux expulsion at the superconducting transition of a 5 μm-tin particle was detected with a signal-to-noise ratio of about 10^5 in a 1 Hz bandwidth.

This device has potential applications in the study of temperature dependent susceptibility as well as of magnetic fluctuations in thin-films and small particles with dimensions that extend into the submicron region.

3.3. Radiofrequency Amplifier

Although most SQUIDs have been used at signal frequencies of no more than a few tens of kilohertz, in the absence of a flux-locked loop they can be operated at much higher frequencies. We briefly describe the design and performance of a tuned SQUID amplifier that has been operated at frequencies up to 100 MHz (31).

When a SQUID is used as an amplifier, it is necessary to take into account not only the voltage across the SQUID, but also the current noise circulating in the SQUID loop which induces a voltage noise in the input circuit (19). The two noise sources are partially correlated (32). To make a tuned amplifier, one connects the signal source in series with a resistance, R_i, a capacitance, C_i, and the input coil of the SQUID, with inductance L_i. It can be shown that optimal performance is achieved when $\alpha^2 Q = 1$, where $Q = \omega L_i/R_i$. Thus, in contrast to the case of untuned input circuits, optimal sensitivity may require α^2 to be rather small, for example, 0.01 for $Q = 100$. In the weakly coupled limit $\alpha^2 \ll 1$ the noise temperature of the amplifier at resonance takes the optimum value (19)

$$T_N = \omega T (S_V S_J)^{1/2}/V_\phi . \qquad (4)$$

where $\omega = 2\pi f$ is the signal frequency. The noise temperature represents the temperature to which R_i would have to be raised to produce a Johnson noise equal to the noise of the amplifier.

We note in passing that measurement theory (33) imposes a lower limit on the noise temperature of any linear amplifier, namely $T_N \geq hf/k_B \ln 2$. As noted previously, it is T_N, rather than ϵ/1Hz, to which fundamental limitations apply (6,7).

The experiments were performed with a SQUID of the type shown in Fig. 3 with a 4-turn input coil. A low effective value of α^2 was achieved by connecting an inductance L_i' in series with L_i so that $Q\alpha^2/(1 + L_i'/L_i) = 1$. At 4.2K and at the resonant frequency of 93 MHz the measured gain was about 16 dB, and the noise temperature was 1.7 ± 0.5K. The noise temperature was within a factor of 2 of the prediction of Eq. (4).

4. APPLICATIONS OF SQUIDS

Both dc and rf SQUIDs have been used for many years in laboratory-based cryogenic measure-

ments. One application is to measure tiny quasistatic voltages arising, for example, from Hall effects, thermoelectric effects, flux creep in superconductors, or quasiparticle charge imbalance in superconductors. Another major application has been the measurement of magnetic susceptibility over a wide range of temperatures. A number of experiments have been performed to measure the static magnetization induced by nuclear magnetic resonance (NMR) or electron spin resonance. With the advent of SQUID amplifiers operating at radio frequencies, it should now be possible to perform NMR measurements at frequencies of 10's to 100's of MHz. Yet another area of application is to standards -- for example in comparing the Josephson volt with other sources of emf, in determining the fundamental constant ratio h/m, and in noise thermometry.

However, SQUIDs have long since left the cryogenics laboratory and have been used in a wide variety of measurements of phenomena that are unrelated to cryogenic environments. An area of rapidly growing importance is biomagnetism: for example, magnetocardiology, the study of spontaneous or evoked brain activity, the detection and location of magnetic particles in the human body, the determination of eye movements, and even the detection of a signal propagating in a single nerve, a squid giant axon. Another major area is geophysics, in which it is often necessary to use SQUIDs under difficult conditions in remote areas. Applications here include magnetotellurics, which involves the determination of the resistivity of the ground using naturally occurring magnetic and electric fluctuations, airborne magnetic gradiometry, gravity gradiometry, rock magnetism, paleomagnetism, piezomagnetism, tectonomagnetism, the mapping of hydrofractures for geothermal energy and enhanced gas recovery, and the detection of internal ocean waves. A quite different realm of sensitive measurement is in various tests of fundamental physical theories, for example, gravity wave antennas, magnetic monopole detectors, and an orbiting gyro test of general relativity.

To illustrate these widespread applications, we briefly discuss just two of them that benefit greatly from the increases in sensitivity offered by the dc SQUID, namely noise thermometry and gravity wave antennas.

4.1. Noise Thermometry

The Johnson noise in a resistance r, which has a spectral density $4k_BT/r$, has been used as an absolute thermometer at temperatures down to a few milliKelvin (34,35). The only major disadvantage of this technique has been the very long averaging time required to achieve high accuracy, particularly at the lowest temperatures. The advent of high sensitivity dc SQUIDs, however, offers the possibility of a dramatic reduction in the averaging time.

If one measures the Johnson noise in a bandwidth Δf for a time t_m, the rms statiscal error, δ, is approximately $(2\Delta f t_m)^{-1/2}$ (34). Clearly, for a given value of δ, one can reduce t_m by increasing Δf correspondingly. The maximum bandwidth, however, is determined by the sensitivity of the SQUID used to measure the Johnson noise. For the dc SQUID in the configuration of an untuned amplifier (i.e. with a resistor r connected directly across the input coil), the noise temperature is given approximately by (19) $T_N = \eta T_s \Delta f$, where ηT_s is proportional to ϵ/1Hz and T_s is the temperature of the SQUID. The bandwidth Δf extends from just above the 1/f noise region, typically a few hertz, to an upper cutoff frequency that is essentially equal to Δf. We assume that we wish to determine a temperature T_o with a noise contribution from the SQUID no greater than δT_o. We thus require $T_N = \eta T_s \Delta f \lesssim \delta T_o$, that is, $\Delta f \lesssim \delta T_o / \eta T_s$. If we combine this expression for bandwidth with the expression for the rms statistical error, we find

$$t_m \gtrsim \eta T_s / 2 T_o \delta^3. \qquad (5)$$

We suppose that $T_s = 1K$, even though the thermometer may be cooled to substantially lower temperatures: The effective temperature of the SQUID may well be set at $\sim 1K$ by the preamplifier that follows it. For the SQUID illustrated in Fig. 3, a measured value of ηT_s is then 6×10^{-9}K sec. If we wish to measure a temperature $T_o = 1$ mK with an error of 1% from both the statistical fluctuations and the SQUID noise ($\delta = 10^{-2}$), we find $t_m > 3$ sec. The corresponding measurement bandwidth is 3 kHz. This measurement time represents a reduction of three orders of magnitude over that reported in the original work on noise thermometers (34). We note that t_m is proportional to ϵ/1Hz, so that the reduction in t_m arises directly from the reduction in noise energy.

4.2 Gravitational Wave Detectors

One application in which a quantum-limited SQUID will ultimately be needed is as part of the transducer in resonant-mass gravitational wave detectors. A number of groups around the world are constructing and/or operating detectors of this type, and I will briefly describe the Stanford version, which is the most sensitive detector currently in operation (36).

The Stanford antenna consists of a cylindrical bar of Al of mass M = 4,800 kg and length ℓ = 3m maintained at 4.2K. The fundamental longitudinal mode of oscillation is at $\omega_a/2\pi = 842$ Hz, and the Q-value has been as high as 5×10^6. A gravitational wave excites longitudinal oscillations in the bar, which are detected by means of the transducer shown in Fig. 6. A thin, circular diaphragm made of Nb is clamped at its perimeter to one end of the bar. Two flat, spiral niobium coils are mounted one on each side of the diaphragm, and connected in paral-

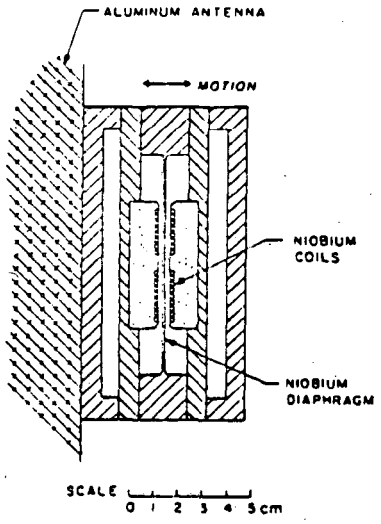

FIGURE 6
Superconducting transducer for gravitational wave detector (from Ref. 36).

lel with the input coil of a SQUID. By means of heat switches, one can store a persistent supercurrent in the loop formed by the two spiral coils. The magnetic fields exert a restoring force on the diaphragm so that, by varying the value of the persistent current, one may adjust the resonant frequency of the diaphragm to be exactly equal to that of the bar. A longitudinal movement of the bar induces a displacement in the diaphragm relative to the two spiral coils, causing an imbalance in their inductance. As a result, a current proportional to the displacement flows through the input coil of the SQUID.

The present antenna has a rms strain sensitivity $\delta\ell/\ell$ of 10^{-18} ($\delta\ell$ is the longitudinal displacement). Although this sensitivity, which is set by thermal noise, is obviously very impressive, it is sufficient to detect only relatively rare events. Thus, there is a very strong motivation to make major improvements in sensitivity. The limit of strain resolution imposed by the zero point longitudinal motion of the bar is $\langle(\delta\ell)^2\rangle^{1/2}/\ell \sim 3 \times 10^{-21}$. At first sight, one might expect that one would have to cool the bar to an absurdly low temperature to achieve the quantum limit, since a frequency of 842 Hz corresponds to a temperature of $\hbar\omega_a/k_B = 40$ nK. However, with proper design, the effective noise temperature of the antenna, T_{eff}, may be much lower than the temperature of the bar, T. For example, if a gravitation signal in the form of a pulse of length τ_s interacts with the bar which has a decay time $\tau_a = Q_a/\omega_a$, it can be shown that (37,38)

$$T_{eff} = T\tau_s/\tau_a = T(\omega_a/Q_a)(2\pi/\Delta\omega), \qquad (5)$$

where $\Delta\omega = 2\pi/\tau_s$ is the bandwidth. Thus, provided Q_a and $\Delta\omega$ are sufficiently large, T_{eff} becomes much less than T. To obtain the quantum limit, we set $T_{eff} = \hbar\omega_a/k_B$, and find that we require $Q_a(\Delta\omega_a/2\pi) \geq k_B T/\hbar$. If one can cool the bar to (say) 10 mK, this inequality can be satisfied with $Q_a = 5 \times 10^6$ and $\Delta\omega_a/2\pi = 300$.

It will obviously take an enormous effort to operate a detector at 10 mK and to reduce parasitic vibrational noise to the required level. However, assuming that such a system can be constructed, it will be necessary to use a quantum limited SQUID amplifier to detect the motion induced by a gravitational wave. Existing SQUID amplifiers that can be coupled effectively to inductances of about 1 μH are roughly two orders of magnitude away from the quantum limit when operated in the He^4 temperature range. It is possible that by cooling such SQUIDs to 10 mK one can achieve near-quantum limited performance, although the problems of 1/f noise and heating at milliKelvin temperatures are both unknown quantities.

In addition to the need to improve the sensitivity of individual gravitational wave detectors to the quantum limit [or even beyond, using the technique of quantum nondemolition (39)], it is essential to operate several detectors in coincidence. Coincidence operation enables one to reduce the noise in any one detector by a large factor (36). The need to develop a quantum-limited SQUID amplifier for this application remains an intriguing challenge.

5. CONCLUDING REMARKS

In this short review, I have tried to show how the fundamental understanding of the noise process in the dc SQUID and the availability of thin-film lithographic techniques have made possible a major advance in sensitivity. I have described three examples of the kind of instrument that one can now fabricate, given suitable photolithographic facilities, but, obviously, I have had to omit many other ingenious and useful devices. Finally, I have given a partial list of the enormous range of measurements to which SQUIDs have been applied, illustrating them with two particular examples where the improved sensitivity is having a major impact. One may hope that these thin-film devices will become available commercially in the not-too-distant future, thereby expanding the scope of their applications even more.

ACKNOWLEDGEMENTS

Parts of the work described were carried out at Berkeley over the past ten years or so, and I wish to express my grateful thanks to Wolf Goubau, Gil Hawkins, Claude Hilbert, Mark

Ketchen, Roger Koch, John Martinis, Claudia Tesche, Dale Van Harlingen and Frederick Wellstood for their dedicated efforts. I have also enjoyed fruitful collaborations with Gordon Donaldson, Robin Giffard, Bob Laibowitz, Colin Pegrum, Stan Raider, and Dick Voss. I thank Peter Michelson for helpful discussions on gravitational wave detectors. I am grateful to Eric Ganz and John Mamin for a critical reading of the manuscript.

This work was supported by the Director, Office of Energy Research, Office of Basic Energy Sciences, Materials Sciences Division of the U.S. Department of Energy under Contract Number DE-AC03-76SF00098.

REFERENCES

(1) R.C. Jaklevic, J. Lambe, A.H. Silver, and J.E. Mercereau, Phys. Rev. Lett. 12 (1964) 159.
(2) J.E. Zimmerman, P. Thiene, and J.T. Harding, J. Appl. Phys. 41 (1970) 1572.
(3) B.D. Josephson, Phys. Lett. 1 (1962) 251.
(4) J. Clarke, W.M. Goubau, and M.B. Ketchen, J. Low Temp. Phys. 25 (1976) 99.
(5) C.D. Tesche and J. Clarke, J. Low Temp. Phys. 29 (1977) 301.
(6) R.H. Koch, D.J. Van Harlingen, and J. Clarke, App. Phys. Lett. 38 (1981) 380.
(7) V.V. Danilov, K.K. Likharev, and A.B. Brown, IEEE Trans. Magn. MAG-19 (1983) 572.
(8) J.H. Greiner, C.J. Kircher, S.P. Klepner, S.K. Lahiri, A.J. Warnecke, S. Basavaiah, E.T. Yen, J.M. Baker, P.R. Brosious, H.-C. Huang, M. Murakami, and I. Ames, IBM J. of Res. and Dev. 24 (1980) 195.
(9) R.H. Koch and J. Clarke, Bull. Am. Phys. Soc. 24 (1979) 264.
(10) R.F. Voss, R.B. Laibowitz, S.I. Raider, and J.Clarke, J. Appl. Phys. 51 (1980) 2306.
(11) M.B. Ketchen and R.F. Voss, Appl. Phys. Lett. 35 (1979) 812.
(12) R.F. Voss, R.B. Laibowitz, A.N. Broers, S.I. Raider, C.M. Knoedler, and J.M. Viggiano, IEEE Trans. Magn. MAG-17 (1981) 395.
(13) M.W. Cromar and P. Carelli, Appl. Phys. Lett. 38 (1981) 723.
(14) M.B. Ketchen and J.M. Jaycox, Appl. Phys. Lett. 40 (1982) 736.
(15) P. Carelli and V. Foglietti, J. Appl. Phys. 53 (1982) 7593.
(16) D.J. Van Harlingen, R.H. Koch, and J. Clarke, Appl. Phys. Lett. 41 (1982) 197.
(17) J.M. Martinis and J. Clarke, IEEE Trans. Magn. MAG-19 (1983) 446.
(18) V.J. de Waal, P. van der Hamer, and J.E. Mooij, SQUID 80, Superconducting Quantum Interference Devices and their Applications, eds. H.D. Hahlbohm and H. Lübbig (Walter de Gruyter, Berlin, 1980) p.391.
(19) J. Clarke, C.D. Tesche, and R.P. Giffard, J. Low Temp. Phys. 37 (1979) 405.
(20) F. Dettman, W. Richter, G. Albrecht, and W. Zahn, Phys. Stat. Sol. (a) 51 (1979) K185.
(21) F. Wellstood, C. Heiden, and J. Clarke, Rev. Sci. Instrum. 55 (1984) 952.
(22) R.H. Koch, Noise in Physical Systems and 1/f Noise, eds. M. Savelli, G. Leroy, and J.P.-Nougier (North-Holland, Amsterdam, 1983) p.377.
(23) C.T. Rogers and R.A. Burhman, IEEE Trans. Magn. MAG-19 (1983) 453.
(24) R.H. Koch, J. Clarke, W.M. Goubau, J.M. Martinis, C. Pegrum, and D.J. Van Harlingen, J. Low Temp. Phys. 51 (1983) 207.
(25) C.D. Tesche, K.H. Brown, A.C. Callegari, M. M. Chen, J.H. Greiner, H.C. Jones, M.B. Ketchen, K.K. Kim, A.W. Kleinsasser, H.A. Notarys, G. Proto, R.H. Wang, and T. Yogi, Proc. LT17.
(26) G.L. Romani, Proc. LT17.
(27) M.B. Ketchen, W.M. Goubau, J. Clarke, and G.B. Donaldson, J. Appl. Phys. 49 (1978) 4111.
(28) V.J. de Waal, T.M. Klapwijk, and P. van den Hamer, J. Low Temp. Phys. 53 (1983) 287.
(29) P. Carelli and V. Foglietti, J. Appl. Phys. 54 (1983) 6065.
(30) M.B. Ketchen, T. Kopley, and H. Ling, Appl. Phys. Lett. 44 (1984) 1008.
(31) C. Hilbert and J. Clarke, to appear in Proc. 1984 Applied Superconductivity Conf.
(32) C. Tesche and J. Clarke, J. Low Temp. Phys. 37 (1979) 397.
(33) C.M. Caves, Phys. Rev. D 26 (1983) 1817.
(34) R.A. Webb, R.P. Giffard, and J.C. Wheatley, J. Low Temp. Phys. 13 (1973) 383.
(35) R.A. Kamper and J.E. Zimmerman, J. Appl. Phys. 42 (1971) 132.
(36) M. Bassan, W.M. Fairbank, E. Mapoles, M.S. McAshan, P.F. Michelson, B. Moskowitz, K. Ralls, and R.C. Taber, Proc. Third M. Grossman Meeting on General Relativity, ed. Hu Ning (Science Press and North-Holland, 1983) p.667.
(37) R.P. Giffard, Phys. Rev. D 14 (1976) 2478.
(38) P.F. Michelson and R.C. Taber, Phys. Rev. D 29 (1984) 2149.
(39) V.B. Braginsky, in Topics in Theoretical and Experimental Astrophysics, eds. V. de Sabbata and J. Weber (Plenum, New York and London, 1977).

TECHNICAL INFORMATION DEPARTMENT
LAWRENCE BERKELEY LABORATORY
UNIVERSITY OF CALIFORNIA
BERKELEY, CALIFORNIA 94720